



This is a repository copy of *Influence of femoral component design on proximal femoral bone mass after total hip replacement : a randomized controlled trial.*

White Rose Research Online URL for this paper:
<https://eprints.whiterose.ac.uk/167436/>

Version: Accepted Version

Article:

Slullitel, P.A., Mahatma, M.M., Farzi, M. et al. (3 more authors) (2021) Influence of femoral component design on proximal femoral bone mass after total hip replacement : a randomized controlled trial. *Journal of Bone and Joint Surgery*, 103 (1). pp. 74-83. ISSN 0021-9355

<https://doi.org/10.2106/jbjs.20.00351>

© 2020 by The Journal of Bone and Joint Surgery. This is an author-produced version of a paper subsequently published in JBJS. Uploaded in accordance with the publisher's self-archiving policy.

Reuse

Items deposited in White Rose Research Online are protected by copyright, with all rights reserved unless indicated otherwise. They may be downloaded and/or printed for private study, or other acts as permitted by national copyright laws. The publisher or other rights holders may allow further reproduction and re-use of the full text version. This is indicated by the licence information on the White Rose Research Online record for the item.

Takedown

If you consider content in White Rose Research Online to be in breach of UK law, please notify us by emailing eprints@whiterose.ac.uk including the URL of the record and the reason for the withdrawal request.



eprints@whiterose.ac.uk
<https://eprints.whiterose.ac.uk/>

How Does Femoral Component Design Influence Proximal Femoral Bone Mass After Total Hip Replacement? A Randomized Controlled Trial

*Pablo A. Slullitel, MD¹

*Mohit M. Mahatma, MRes²

Mohsen Farzi, PhD³

George Grammatopoulos, BSc (Hons), MBBS (Hons), DPhil (Oxon), MRCS (Eng), FRCS
(Tr & Orth)¹

*J Mark Wilkinson, PhD, FRCS (Tr&Orth)²

*PE Beaulé, MD, FRCSC¹

¹Division of Orthopaedic Surgery, The Ottawa Hospital, Ottawa, Canada, ²Department of Oncology and Metabolism, University of Sheffield, Sheffield, UK, ³Centre for Computational Imaging and Simulation Technologies in Bioscience, University of Leeds, Leeds, UK

*Equal contribution

Correspondence to:

P Beaulé, Division of Orthopaedic Surgery, The Ottawa Hospital - General Campus, 501 Smyth Road, CCW 1640, Ottawa, Ontario, Canada K1H 8L6. Email: pbeaule@toh.ca

JM Wilkinson, Department of Oncology and Metabolism, The Medical School, Beech Hill Road, Sheffield, S102TN, United Kingdom. Email: j.m.wilkinson@sheffield.ac.uk

Author contributions

PA Slullitel: Conducted data analysis, Wrote the manuscript

MM Mahatma: Conducted data analysis, Wrote the manuscript

M Farzi: Assisted with data analysis, Edited the manuscript

G Grammatopoulos: Assisted with data analysis, Edited the manuscript

JM Wilkinson: Co-designed the study, Led data analysis, Wrote the manuscript

PE Beaulé: Led and co-designed the study, Led patient recruitment, Edited the manuscript

Funding statement

The project was funded by Johnson & Johnson Medical Products and Synthes Canada Ltd. (d.b.a. DuPuy Synthes). The funder manufactures all of the prostheses studied in this work, took no part in the design or conduct of the trial, analysis or interpretation of the results or preparation of the manuscript.

Ethical review statement

The trial was approved by Ottawa Hospital Institutional Review Board (OHSN-REB 2010913-01H) and registered with clinicaltrials.gov (NCT01558752).

3 **Abstract**

4 **Aims**

5 In this randomized **controlled** trial (**RCT**), we aimed to compare post-operative bone
6 remodeling and bone turnover over 2 years following total hip arthroplasty using the short,
7 proximally-coated Tri-Lock ‘Bone-Preserving Stem’ versus a conventional, fully-coated
8 Corail prosthesis.

9 **Methods**

10 Forty-six participants received the Tri-Lock prosthesis and 40 received the Corail. At
11 baseline, both groups had similar demographics, proximal femoral bone mineral density
12 (BMD), bone turnover markers, radiographic canal flare index, and patient-reported
13 outcome measure scores. Outcomes were **measured** at week 26, 52, and 104.

14 **Results**

15 Loss in periprosthetic bone, measured by high sensitivity Dual-energy X-ray
16 Absorptiometry Region Free Analysis (DXA-RFA) was identified at the calcar and
17 proximal lateral femur in both prosthesis groups ($p < 0.05$). However, the conventional
18 prosthesis demonstrated a smaller reduction in BMD versus the bone-preserving prosthesis
19 ($p < 0.001$). This effect was most prominent in the region of the femoral calcar **and greater**
20 **trochanter**. A small gain in BMD was also identified in some areas **that was greater** with
21 the **conventional versus the bone-preserving prosthesis** ($p < 0.001$). Both groups
22 experienced similar changes in bone turnover markers and improvement in PROMs scores
23 over the study period ($p > 0.05$). **The** adverse event rate was **also** similar between groups
24 (**$p > 0.05$**).

25 **Conclusions**

26 This **RCT** shows that prostheses intended to preserve proximal femoral bone do not
27 necessarily perform better in this regard than conventional cementless designs. DXA-RFA
28 is a sensitive tool for detecting spatially-complex patterns of periprosthetic bone
29 remodeling.

30 **Level of Evidence:**

31 **Therapeutic** Level 1

32 **Introduction**

33 Although pooled data from THA case-series and joint registries shows a 25-year
34 prosthesis survivorship of between 58%-78%¹, the burden of periprosthetic femoral fracture
35 after total hip arthroplasty (THA) continues to increase². This observation has prompted the
36 emergence of shorter-stemmed, ‘bone-preserving’ femoral prostheses intended to mitigate
37 the periprosthetic fracture risk and simplify revision surgery. Those advocating for shorter
38 stems argue for reduced femoral bone removal at surgery, reduced strain-adaptive
39 remodeling (stress shielding) within the proximal femur, and tissue-sparing approaches
40 during femoral canal preparation and prosthesis insertion^{3,4}.

41 At prosthesis design, computational modeling techniques such as finite element
42 analysis (FEA) are commonly used to predict and optimize prosthesis-bone construct
43 stability and load transfer characteristics^{5,6}. In order to validate FEA findings in patients, a
44 clinical measure of bone strain-adaptive remodeling is required, and Dual-energy X-ray
45 Absorptiometry (DXA) is typically used for this purpose⁷⁻⁹. However, DXA analysis using
46 the conventional Gruen zone region of interest (ROI) approach has limited ability to resolve
47 spatially-complex patterns of bone remodeling around prostheses¹⁰. **To address this, DXA-**
48 **Region Free Analysis (DXA-RFA) was developed, allowing resolution of bone mineral**
49 **density (BMD) at the individual pixel level¹¹⁻¹⁴ and because it does not average the**
50 **pixel-level data into ROIs, there is no loss of resolution and interpretation variations**
51 **associated with conventional DXA studies¹⁵.**

52 The primary aim of this randomized **controlled** trial (**RCT**) was to determine
53 whether periprosthetic bone loss measured by DXA-RFA over 2-years after THA using the
54 proximally porous-coated and shorter stemmed Tri-Lock “Bone-Preserving Stem” (BPS®)

55 femoral prosthesis (DePuy Synthes, Warsaw, USA) is lower than that occurring around the
56 conventional collarless Corail® prosthesis (DePuy Synthes). We also compared
57 biochemical markers of bone turnover, patient-reported outcome measures (PROMs) and
58 adverse events (AEs) between groups.

59

60 **Materials and Methods**

61 Between May 2013 and May 2017, 2485 patients underwent THA at The Ottawa Hospital
62 **amongst six surgeons. Initial screening eliminated 1927 patients for the following two**
63 **reasons: two surgeons were not participating in the study (n=689); and initial chart**
64 **reviewed by the research team met the exclusion criteria (n=1238). A consecutive**
65 **group of 558** patients were **further interviewed** for eligibility out of which 88 patients
66 with idiopathic osteoarthritis of the hip were recruited to the trial (Figure 1). The trial was
67 IRB-approved, registered with clinicaltrials.gov (NCT01558752), and conducted in
68 accordance with the Declaration of Helsinki. Patients with prior hip surgery, severe femoral
69 bone deficiency, femoral neck fracture, known secondary causes of arthritis, **known**
70 metabolic bone disease and past or present use of drugs known to affect bone metabolism,
71 and patients anticipated to receive contralateral hip surgery within **1-year**, were excluded
72 from the study. Using computer-generated, varied block randomization with allocation
73 concealment, patients were randomized during the preoperative outpatient visit. Treatment
74 allocation was made on a 1:1 basis to receive either the Tri-Lock BPS with a modular
75 cementless porous-coated acetabular component (Pinnacle®, Depuy Synthes) using a
76 metal-on-polyethylene bearing surface, or the Corail® prosthesis with a titanium porous-
77 coated monoblock shell (DeltaMotion®, Depuy Synthes) using a ceramic-on-ceramic

78 bearing surface. **The Tri-Lock “Bone-Preserving Stem” (BPS®) femoral prosthesis**
79 **(DePuy Synthes, Warsaw, USA) is a commonly used example of this philosophy.**
80 **Manufactured in TiAl6V4 alloy with a stem length of 95 to 119mm, the Tri-Lock**
81 **prosthesis has a thin tapered-wedge geometry with a reduced lateral shoulder and**
82 **GRIPTION® porous titanium coating in its proximal (metaphyseal) section (pore size**
83 **300 microns, volume porosity 80%) that is designed to closely fit the proximal**
84 **femoral metaphysis and promote osseointegration. The prosthesis is inserted with a**
85 **bone-cutting broach. The Corail is also a tapered-wedge stem composed of the same**
86 **TiAl6V4 alloy, but with a more conventional geometry and is fully hydroxyapatite-**
87 **coated (HA thickness 155 microns, pore size 250 microns, volume porosity 75%). The**
88 **Corail is inserted using a compaction broach.** After randomization, two patients
89 allocated to the Corail group received an alternate implant as the femoral canal was deemed
90 by the surgeon to be not suitable for the Corail prosthesis and were excluded from further
91 study. The participant and allied health providers remained blinded to treatment group
92 allocation until after the final study visit (2-years).

93 **Surgical technique.** In all, 46 patients received the Tri-Lock prosthesis and 40 received the
94 Corail. Each prosthesis was inserted according to its specific manufacturer’s instructions
95 and design philosophy. Four surgeons performed the procedures, each using their preferred
96 surgical approach. In the Tri-Lock group 33 were performed using the anterior approach, 6
97 lateral, 1 posterior, and 6 posterolateral; and for the Corail 26 were anterior, 8 lateral, 1
98 posterior, and 5 posterolateral (chi-squared = 0.792, p=0.851). Postoperatively, immediate
99 full weight-bearing was allowed using crutches. Routine postoperative thromboembolic

100 prophylaxis consisted of 5 days of 10mg rivaroxaban daily, followed by 25 days of 81mg
101 aspirin daily.

102 **Outcome measures and monitoring.** All DXA scan acquisitions were made using the
103 same GE Lunar iDXA densitometer (GE Healthcare Lunar, Madison, WI) in ‘orthopaedic’
104 scan mode and using a standard acquisition protocol¹⁶. Scans were made at post-operative
105 baseline (within 2-weeks of surgery), and at weeks 26, 52 and 104 postoperatively.
106 Analysis of the acquired pixel-level bone maps was made using the ‘Encore’ windows-
107 based user interface (GE Healthcare) and implemented in Matlab v9.5 R2018b (Mathworks
108 Inc, Cambridge, MA). Each image was composed of approximately 10,000 pixels (each
109 0.60mmx0.60mm in size), and analyzed according to a previously described protocol¹³. A

110 **post-operative baseline conventional BMD measurement of the contralateral native**
111 **hip (without THA) was also made to assess for evidence of pre-existing osteoporosis.**

112 Biochemical markers of bone turnover were measured from morning-fasting serum samples
113 taken at pre-operative baseline and at weeks 12, 26, 52 and 104. Carboxy-terminal
114 telopeptide of type I collagen (CTX), a marker of type-I collagen resorption, was measured
115 by electrochemiluminescent assay (β -CrossLaps, Elecsys, Roche Diagnostics,
116 Indianapolis, USA). Intact amino-terminal propeptide of type I procollagen (PINP), a
117 marker of type-I collagen formation, was also measured using the Elecsys system.

118 Plain radiographic assessments using anteroposterior pelvic and lateral radiographs,
119 were made post-operatively and at weeks 12, 26, 52, and 104. Differences between
120 preoperative and postoperative global offset, as well as leg length discrepancy, were
121 measured by an arthroplasty surgeon, following previously described methods⁷. The canal
122 flare index was measured as per Boyle et al.¹⁷ (stovepipe<3, normal 3-4.7, champagne flute

123 >4.7-6.5). Stem alignment was measured and grouped in varus ($\geq +1^\circ$), neutral
124 ($< +1^\circ / > -1^\circ$) and valgus position ($\leq -1^\circ$). Characterization of lucencies and bone
125 resorption was based on the zones described by Gruen with a slight modification for the
126 short stem¹⁸. Non-progressive periprosthetic lucencies of <2mm, outlined by a thin sclerotic
127 line, were considered as normal⁸.

128 PROMs assessments and recording of AEs were made on the same day as the
129 radiological assessments. PROMs included the modified Harris Hip Score (mHHS)¹⁹, the
130 Western Ontario and McMaster University Osteoarthritis Index (WOMAC)²⁰ score and the
131 University of California, Los Angeles (UCLA) activity scale²¹.

132

133 **Statistical analysis.** All analyses were made ‘per-protocol’ using two-tailed testing and a
134 critical p-value of 0.05. Categorical data was analyzed using the **chi-squared** test.
135 Continuous data were analyzed parametric and non-parametric tests, as appropriate to each
136 dataset distribution. **Longitudinal continuous data was analyzed by repeated-measures**
137 **ANOVA. For DXA-RFA, these analyses were made after** correction for multiple testing
138 by False Discovery Rate (FDR)¹⁴, **and** denoted as q-values (**with** $q \leq 0.05$ considered
139 statistically significant). The power calculation was based upon data for cementless femoral
140 prostheses assuming a between-group difference in Gruen zone 7 of 0.14g/cm² (10%,
141 standard deviation 0.23) by conventional DXA analysis, giving a sample size of 43
142 participants per group for 80% power at the 5% significance level.

143

144 **Source of Funding**

145 The project was funded by Johnson & Johnson Medical Products and Synthes
146 Canada Ltd. (d.b.a. DuPuy Synthes). The funder manufactures all prostheses studied in this

147 work, took no part in the design or conduct of the trial, analysis or interpretation of the
148 results or preparation of the manuscript.

149

150 **Results**

151 A total of 47 females and 39 males with a mean age of 59.4 ± 10.6 years old
152 completed follow-up (98% of subjects randomized) and were included in the analysis.
153 Patients in the Tri-Lock group (n=46) were of similar age, sex, body mass index (BMI) as
154 those on the Corail group (n=40, Table 1, $p > 0.05$ all comparisons). **BMD of the**
155 **contralateral native proximal femur was also similar between groups and within the**
156 **normal expected reference ranges (BMD, t- and z-scores $p > 0.05$ all comparisons).**
157 There were more patients in American Society of Anaesthesia (ASA) class III in the Tri-
158 Lock versus the Corail group ($p = 0.049$).

159 At immediate post-operative baseline, the distribution of periprosthetic BMD was
160 similar between groups (Figure 2). **Subsequent bone loss around both prostheses was**
161 **observed in the area of the calcar and in a cancellous area of the distal greater trochanter**
162 **(Figure 3). Bone loss was significantly greater in the Tri-Lock group versus the Corail**
163 **over the 2-year study period and observed at all interval timepoints (ANOVA**
164 **$p < 0.0001$, Table 2). Small areas of significant bone gain were also observed over the**
165 **follow up period that was broadly but sparsely distributed for both prosthesis types**
166 **(Figure 3). This gain was initially more apparent in the inferior lesser trochanter in**
167 **the Tri-Lock group ($p < 0.001$), but over the full study period was greater in the Corail**
168 **group (Table 2 ANOVA $p < 0.001$).**

169 At pre-operative baseline, serum values for the bone resorption marker CTX and the
170 bone formation marker PINP were similar ($P > 0.05$ both comparisons, Table 1). Post-

171 operatively both bone turnover markers underwent a transient increase, peaking at week 26,
172 before returning to baseline by week 52 (Figure 4). No between-group differences in bone
173 turnover markers were identified (ANOVA, $p>0.05$ both comparisons).

174 At preoperative radiological assessment, the mean canal flare index was 3.92 ± 0.6 ,
175 and was similar between groups ($p=0.549$). On immediate post-operative radiographs, the
176 prosthesis was positioned in greater varus in the Corail versus the Tri-Lock group (mean
177 2.07° versus 0.78° $p=0.001$ Table 3). Other radiographic parameters were similar between
178 groups. Non-progressive, $<2\text{mm}$ lucent lines were detected in zones 1 and 7 of one Tri-
179 Lock stem and in the same zones of three Corail stems. No cases had evidence of femoral
180 component loosening.

181 Patients in both treatment groups had similar mHHS, WOMAC and ULCA scores
182 at pre-operative baseline ($p>0.05$ all comparisons, Table 4). Both groups experienced
183 similar improvements in all PROM scores at week 104, with no difference in the change
184 scores between groups. There were 8 AEs in the Tri-Lock group and 5 in the Corail group
185 ($p=0.741$). **This included 3 (7.5%) calcar cracks in the Corail group and 1 (2.17%) in**
186 **the Tri-Lock group; 1 (2.5%) deep infection in the Corail group; 1 (2.2%) femoral**
187 **nerve palsy in the Tri-Lock group; and 6 episodes of postoperative thigh pain at the**
188 **latest follow-up (5 [10.9%] in the Tri-Lock group and 1 [2.5%] in the Corail).** One
189 case (2.2%) in the Tri-Lock group developed aseptic loosening and underwent revision
190 surgery with a non-modular, distally-fixed, conical stem at week 96.

191 We used linear regression analysis to explore the relationships between the area of
192 greatest bone loss within the proximal medial femur and possible predictive factors,
193 including age, sex, radiographic and PROMs variables. Although a correlation matrix
194 suggested a relation between prosthesis alignment and BMD change at week 104 (Pearson

195 $r= 0.386$, $p<0.001$), this was entirely accounted for by prosthesis group. In the final
196 regression model, only prosthesis group remained a significant predictor of bone loss in the
197 proximal medial femur (adjusted $r^2= 0.063$, $\text{Beta}=7.591$ (standard error= 2.996); $p=0.013$),
198 with greater loss for the Tri-Lock prosthesis.

199

200 **Discussion**

201 The goal of modern joint arthroplasty is to create a prosthesis-host construct that
202 provides predictable pain relief and restores function, whilst causing the minimal possible
203 disruption to the local biological environment¹⁸. The emergence of shorter “bone-
204 preserving” femoral prostheses **follows** that philosophy, but the effect **of these prostheses**
205 on the local bone environment in the patient remains unclear²² **and is mainly based on**
206 **FEA modeling**^{17, 23-26}. In this 2-year RCT, **both the Tri-Lock BPS and CORAIL** designs
207 resulted in only a modest disturbance of the natural patterns of strain-adaptive remodeling
208 of the proximal femur, and both performed similarly in terms of plain radiographic
209 **outcomes, PROMs and AE rates. Both designs are tapered wedges made from the**
210 **same titanium alloy, but differ in stem length, geometry, extent and type of surface**
211 **coating, and fixation philosophy (3-point fixation versus conventional taper)**. However,
212 contrary to our anticipated results, we found better bone conservation around the
213 conventional prosthesis than the proposed bone-preserving one.

214 **In a post-mortem study**, Engh²⁷, demonstrated the effect of prosthesis stiffness on
215 the local bone environment **and whereby short stems would load the proximal femur in**
216 **a more physiological way, therefore preventing future stress shielding. Several**
217 **authors have studied this looking at a variety of stem designs with mixed results**
218 **(Table 5)**²⁸⁻³². However, given the diversity of conventional and short stems available

219 **in the market and each with different load-sharing philosophies²², our results cannot**
220 **be extrapolated to other designs that were not subjected to a similar high-resolution**
221 **DXA-RFA analysis. Similarly, canal preparation technique may also affect**
222 **periprosthetic bone remodeling. In the non-destructive clinical setting, Hjorth et al**
223 **compared** compaction versus standard broaching when implanting the same Bi-Metric
224 stem, **and** found only minor BMD differences in favor of compaction at 1- and 5-years³³.
225 **Their study used conventional DXA analysis that was not able to resolve the implant-**
226 **bone interface. Using DXA-RFA we resolved events at pixel level at this interface and**
227 **found no substantial difference between the implant groups to suggest a meaningful**
228 **effect of broaching technique on the initial periprosthetic interface BMD. Further,**
229 **given that the post-operative changes in BMD between the groups were not**
230 **differentially located at the implant-bone interface, we conclude that the differences in**
231 **broaching technique between the groups was not a significant contributor to the**
232 **observed BMD outcomes.**

233 Modern imaging approaches, such as computational tomography and magnetic
234 resonance imaging, also provide cross-sectional detail at high-resolution. However, despite
235 advances in metal-reduction sequences, **challenges due to beam hardening, metal**
236 **susceptibility artifacts and other issues remain that limit their application when**
237 **studying events at or near the implant-bone interface³⁴⁻³⁶. DXA-RFA applied here,**
238 **apart from not suffering artifact limitations to the same extent, uses advanced**
239 computer vision algorithms to resolve bone architecture including events at the implant-
240 bone interface¹⁵, and allows study of any prosthesis geometry without the resolution and
241 sampling limitations of ROI-based analysis^{37, 38}. **However, as each prosthesis and its**
242 **canal preparation technique (i.e. different broach designs) are not separable, we were**

243 **unable to comment directly on the independence of each element on the overall**
244 **observed bone remodeling effects.**

245 Our study also has limitations. **The inclusion of different bearing surface couple**
246 **for each femoral prosthesis may be considered as a potential confounding factor in**
247 **respect of axial load transferred to the proximal femur. However, in the design of this**
248 **study we did not consider this to be a material issue, based upon previous literature**
249 **addressing this question. In 2007, Kim et al reported the results of an RCT in which**
250 **50 subjects undergoing simultaneous, bilateral, cementless THA received an alumina-**
251 **on-alumina bearing in one hip and an alumina-on-polyethylene in the other, finding**
252 **no differences in proximal femoral periprosthetic BMD between the bearing couples**
253 **over 5 years³⁹.**

254 The 2-year timeframe does not reflect the service life of the prosthesis. However,
255 this study was constructed to quantitate the effect of each prosthesis philosophy on bone
256 remodeling **over the period when these changes are most dynamic.** Our biochemical
257 marker data confirmed that **the major phase of prosthesis-related** bone remodeling is
258 complete within the **2-year** timeframe used in this study (return of markers to baseline
259 **bone turnover rates**), and are consistent with previous studies of femoral **strain-adaptive**
260 bone remodeling after THA^{40, 41}. Our biomarker data did not differentiate the prosthesis
261 brands. Serum biomarker data reflect bone turnover events throughout the body. Whilst the
262 observed biomarker changes reflected the surgical event, it is perhaps not surprising that
263 they were insufficiently sensitive to resolve the subtle differences in local bone remodeling
264 observed between the prostheses. DXA-RFA, like all DXA analyses, provides a 2-
265 dimensional composite of 3-dimensional events. However, this is a limitation of DXA itself

266 rather than the RFA-analysis technology that can also be applied to cross-sectional image
267 data.

268 Although modestly different in their bone remodeling characteristics, this trial
269 shows that the Corail prosthesis has more favorable bone remodeling characteristics than
270 the Tri-Lock BPS. However, large-scale clinical data also shows us that design features
271 which facilitate proximal load transfer and reduce early periprosthetic fracture rates do not
272 necessarily perform in the same way later in the prosthesis' service life⁴². Ultimately, long-
273 term periprosthetic fracture and loosening-free prosthesis survival in large clinical series
274 will **determine the clinical significance of more physiological loading of the femur in**
275 **regards to a cementless prosthesis design's overall performance**^{43, 44}.

277 **References**

- 278 1. Evans JT, Evans JP, Walker RW, Blom AW, Whitehouse MR, Sayers A. How long
279 does a hip replacement last? A systematic review and meta-analysis of case series and
280 national registry reports with more than 15 years of follow-up. *Lancet*. 2019 Feb
281 16;393(10172):647-54. Epub 2019/02/21.
- 282 2. Innmann MM, Streit MR, Bruckner T, Merle C, Gotterbarm T. Comparable
283 Cumulative Incidence of Late Periprosthetic Femoral Fracture and Aseptic Stem
284 Loosening in Uncemented Total Hip Arthroplasty-A Concise Follow-Up Report at a
285 Minimum of 20 Years. *J Arthroplasty*. 2018 Apr;33(4):1144-8. Epub 2017/12/17.
- 286 3. Patel RM, Stulberg SD. The rationale for short uncemented stems in total hip
287 arthroplasty. *Orthop Clin North Am*. 2014 Jan;45(1):19-31. Epub 2013/11/26.
- 288 4. Goshulak P, Samiezadeh S, Aziz MS, Bougherara H, Zdero R, Schemitsch EH. The
289 biomechanical effect of anteversion and modular neck offset on stress shielding for
290 short-stem versus conventional long-stem hip implants. *Med Eng Phys*. 2016
291 Mar;38(3):232-40. Epub 2016/01/18.
- 292 5. Huiskes R, Weinans H, van Rietbergen B. The relationship between stress
293 shielding and bone resorption around total hip stems and the effects of flexible
294 materials. *Clinical Orthopaedics and Related Research*. 1992;274:124-34.
- 295 6. Huiskes R. Stress shielding and bone resorption in THA: clinical versus
296 computer-simulation studies. *Acta Orthop Belgica*. 1993;59 Suppl 1:118-29.
- 297 7. Kerner J, Huiskes R, van Lenthe GH, Weinans H, van Rietbergen B, Engh CA, et
298 al. Correlation between pre-operative periprosthetic bone density and post-operative
299 bone loss in THA can be explained by strain-adaptive remodelling. *J Biomech*.
300 1999;32(7):695-703.
- 301 8. Lerch M, Kurtz A, Stukenborg-Colsman C, Nolte I, Weigel N, Bougoucha A, et al.
302 Bone remodeling after total hip arthroplasty with a short stemmed metaphyseal
303 loading implant: finite element analysis validated by a prospective DEXA
304 investigation. *J Orthop Res*. 2012 Nov;30(11):1822-9. Epub 2012/04/20.
- 305 9. ten Broeke RH, Tarala M, Arts JJ, Janssen DW, Verdonschot N, Geesink RG.
306 Improving peri-prosthetic bone adaptation around cementless hip stems: a clinical
307 and finite element study. *Med Eng Phys*. 2014 Mar;36(3):345-53. Epub 2014/01/01.
- 308 10. Gruen TA, McNeice GM, Amstutz HC. Modes of failure of cemented stem-type
309 femoral components. A radiographic analysis of loosening. *Clin Orthop*. 1979;141:17-
310 27.
- 311 11. Morris RM, Yang L, Martin-Fernandez MA, Pozo JM, Frangi AF, Wilkinson JM.
312 High-spatial-resolution bone densitometry with dual-energy X-ray absorptiometric
313 region-free analysis. *Radiology*. 2015 Apr;275(1):310. Epub 2015/03/24.
- 314 12. Farzi M, Pozo JM, McCloskey E, Eastell R, Harvey N, Wilkinson JM, et al. A
315 Spatio-Temporal Ageing Atlas of the Proximal Femur. *IEEE Trans Med Imaging*. 2019
316 Oct 23. Epub 2019/10/28.
- 317 13. Farzi M, Morris RM, Penny J, Yang L, Pozo JM, Overgaard S, et al. Quantitating
318 the effect of prosthesis design on femoral remodeling using high - resolution region -

319 free densitometric analysis (DXA - RFA). *Journal of Orthopaedic Research*.
320 2017;35(10):2203-10.

321 14. Parker AM, Yang L, Farzi M, Pozo JM, Frangi AF, Wilkinson JM. Quantifying
322 pelvic periprosthetic bone remodeling using dual-energy X-ray absorptiometry
323 region-free analysis. *Journal of Clinical Densitometry*. 2017;20(4):480-5.

324 15. Wilkinson JM, Morris RM, Martin-Fernandez MA, Pozo JM, Frangi AF, Maheson
325 M, et al. Use of high resolution dual-energy x-ray absorptiometry-region free analysis
326 (DXA-RFA) to detect local periprosthetic bone remodeling events. *J Orthop Res*. 2015
327 May;33(5):712-6.

328 16. Wilkinson JM, Peel NFA, Elson RA, Stockley I, Eastell R. Measuring bone mineral
329 density of the pelvis and proximal femur after total hip arthroplasty. *J Bone Joint Surg*.
330 2001;83-B(2):283-8.

331 17. Boyle C, Kim IY. Comparison of different hip prosthesis shapes considering
332 micro-level bone remodeling and stress-shielding criteria using three-dimensional
333 design space topology optimization. *Journal of biomechanics*. 2011;44(9):1722-8.

334 18. Knutsen AR, Lau N, Longjohn DB, Ebramzadeh E, Sangiorgio SN. Periprosthetic
335 femoral bone loss in total hip arthroplasty: systematic analysis of the effect of stem
336 design. *Hip International*. 2017;27(1):26-34.

337 19. Harris WH. Traumatic arthritis of the hip after dislocation and acetabular
338 fractures: treatment by mold arthroplasty: an end-result study using a new method of
339 result evaluation. *JBJS*. 1969;51(4):737-55.

340 20. Bellamy N, Buchanan WW, Goldsmith CH, Campbell J, Stitt LW. Validation study
341 of WOMAC: a health status instrument for measuring clinically important patient
342 relevant outcomes to antirheumatic drug therapy in patients with osteoarthritis of the
343 hip or knee. *The Journal of rheumatology*. 1988;15(12):1833-40.

344 21. Zahiri CA, Schmalzried TP, Szuszczewicz ES, Amstutz HC. Assessing activity in
345 joint replacement patients. *The Journal of arthroplasty*. 1998;13(8):890-5.

346 22. Khanuja HS, Banerjee S, Jain D, Pivec R, Mont MA. Short bone-conserving stems
347 in cementless hip arthroplasty. *J Bone Joint Surg Am*. 2014 Oct 15;96(20):1742-52.
348 Epub 2014/10/17.

349 23. Burchard R, Braas S, Soost C, Graw JA, Schmitt J. Bone preserving level of
350 osteotomy in short-stem total hip arthroplasty does not influence stress shielding
351 dimensions - a comparing finite elements analysis. *BMC Musculoskelet Disord*. 2017
352 Aug 7;18(1):343. Epub 2017/08/09.

353 24. Cristofolini L, Juszczak M, Taddei F, Field RE, Rushton N, Viceconti M. Stress
354 shielding and stress concentration of contemporary epiphyseal hip prostheses. *Proc*
355 *Inst Mech Eng H*. 2009 Jan;223(1):27-44. Epub 2009/02/26.

356 25. McNamara BP, Cristofolini L, Toni A, Taylor D. Relationship between bone-
357 prosthesis bonding and load transfer in total hip reconstruction. *Journal of*
358 *biomechanics*. 1997;30(6):621-30.

359 26. van Rietbergen B, Huiskes R. Load transfer and stress shielding of the
360 hydroxyapatite-ABG hip: a study of stem length and proximal fixation. *The Journal of*
361 *arthroplasty*. 2001;16(8):55-63.

362 27. Engh CA, Jr., Sychterz C, Engh C, Sr. Factors affecting femoral bone remodeling
363 after cementless total hip arthroplasty. *J Arthroplasty*. 1999 Aug;14(5):637-44. Epub
364 1999/09/04.

- 365 28. Schilcher J, Ivarsson I, Perlbach R, Palm L. No Difference in periprosthetic bone
366 loss and fixation between a standard-length stem and a shorter version in cementless
367 total hip arthroplasty. A randomized controlled trial. *The Journal of arthroplasty*.
368 2017;32(4):1220-6.
- 369 29. Meyer JS, Freitag T, Reichel H, Bieger R. Periprosthetic Bone Mineral Density
370 Changes After Implantation of a Curved Bone Preserving Hip Stem Compared to a
371 Standard Length Straight Stem: 5-Yr Results of a Prospective, Randomized DXA-
372 Analysis. *Journal of clinical densitometry : the official journal of the International*
373 *Society for Clinical Densitometry*. 2019 Jan-Mar;22(1):96-103. Epub 2018/08/22.
- 374 30. Salemyr M, Muren O, Ahl T, Bodén H, Eisler T, Stark A, et al. Lower
375 periprosthetic bone loss and good fixation of an ultra-short stem compared to a
376 conventional stem in uncemented total hip arthroplasty. *Acta orthopaedica*.
377 2015;86(6):659-66. Epub 2015/07/03.
- 378 31. Freitag T, Hein MA, Wernerus D, Reichel H, Bieger R. Bone remodelling after
379 femoral short stem implantation in total hip arthroplasty: 1-year results from a
380 randomized DEXA study. *Archives of orthopaedic and trauma surgery*. 2016
381 Jan;136(1):125-30. Epub 2015/11/29.
- 382 32. Kim YH, Park JW, Kim JS. Ultrashort versus Conventional Anatomic Cementless
383 Femoral Stems in the Same Patients Younger Than 55 Years. *Clin Orthop Relat Res*.
384 2016 Sep;474(9):2008-17. Epub 2016/06/05.
- 385 33. Hjorth MH, Kold S, Soballe K, Langdahl BL, Nielsen PT, Christensen PH, et al.
386 Preparation of the Femoral Bone Cavity for Cementless Stems: Broaching vs
387 Compaction. A Five-Year Randomized Radiostereometric Analysis and Dual Energy X-
388 Ray Absorption Study. *J Arthroplasty*. 2017 Jun;32(6):1894-901. Epub 2017/01/24.
- 389 34. Jungmann PM, Agten CA, Pfirrmann CW, Sutter R. Advances in MRI around
390 metal. *J Magn Reson Imaging*. 2017 Oct;46(4):972-91. Epub 2017/03/28.
- 391 35. Katsura M, Sato J, Akahane M, Kunimatsu A, Abe O. Current and Novel
392 Techniques for Metal Artifact Reduction at CT: Practical Guide for Radiologists.
393 *Radiographics*. 2018 Mar-Apr;38(2):450-61. Epub 2018/03/13.
- 394 36. Baumann BM, Chen EH, Mills AM, Glaspey L, Thompson NM, Jones MK, et al.
395 Patient perceptions of computed tomographic imaging and their understanding of
396 radiation risk and exposure. *Annals of emergency medicine*. 2011 Jul;58(1):1-7 e2.
- 397 37. Astrakas LG, Argyropoulou MI. Shifting from region of interest (ROI) to voxel-
398 based analysis in human brain mapping. *Pediatr Radiol*. 2010 Dec;40(12):1857-67.
399 Epub 2010/05/14.
- 400 38. Zikou AK, Kitsos G, Tzarouchi LC, Astrakas L, Alexiou GA, Argyropoulou MI.
401 Voxel-based morphometry and diffusion tensor imaging of the optic pathway in
402 primary open-angle glaucoma: a preliminary study. *Am J Neuroradiol*. 2012
403 Jan;33(1):128-34. Epub 2011/11/26.
- 404 39. Kim YH, Yoon SH, Kim JS. Changes in the bone mineral density in the
405 acetabulum and proximal femur after cementless total hip replacement: alumina-on-
406 alumina versus alumina-on-polyethylene articulation. *J Bone Joint Surg Br*. 2007
407 Feb;89(2):174-9. Epub 2007/02/27.
- 408 40. Huang TW, Wang CJ, Shih HN, Chang Y, Huang KC, Peng KT, et al. Bone turnover
409 and periprosthetic bone loss after cementless total hip arthroplasty can be restored

410 by zoledronic acid: a prospective, randomized, open-label, controlled trial. BMC
411 Musculoskelet Disord. 2017 May 22;18(1):209. Epub 2017/05/24.
412 41. Wilkinson JM, Stockley I, Peel NFA, Hamer AJ, Elson RA, Barrington NA, et al.
413 Effect of pamidronate in preventing local bone loss after total hip arthroplasty: A
414 randomized, double-blind, controlled trial. J Bone Miner Res. 2001;16(3):556-64.
415 42. Carli AV, Negus JJ, Haddad FS. Periprosthetic femoral fractures and trying to
416 avoid them: what is the contribution of femoral component design to the increased
417 risk of periprosthetic femoral fracture? Bone Joint J. 2017 Jan;99-B(1 Supple A):50-9.
418 Epub 2017/01/04.
419 43. National Joint Registry for England W, Northern Ireland and the Isle of Man.
420 16th Annual Report. www.njrreports.org.uk: 2019.
421 44. Registry AOANJR. 20th Annual Report. [https://aoanjrr.sahmri.com/annual-](https://aoanjrr.sahmri.com/annual-reports-2019)
422 [reports-2019](https://aoanjrr.sahmri.com/annual-reports-2019): 2019.
423

424 **Acknowledgement**

425 The authors would like to acknowledge Professor AF Frangi, Centre for Computational
426 Imaging and Simulation Technologies in Bioscience, University of Leeds, Leeds, UK, for
427 his contribution to the development of the DXA-RFA methodology and its application in
428 this project. The authors also wish to acknowledge Johanna Dobransky and Cheryl
429 Kreviazuk (Ottawa Hospital Research Institute) for assisting with patient recruitment and
430 data collection.

431 **Legend to figures**

432

433 Figure 1. Consort diagram showing patient selection, treatment allocation and analysis
434 between the prosthesis groups.

435

436 Figure 2. Heatmaps showing baseline pixel-level BMD distribution in each prosthesis
437 group measured by DXA-RFA.

438

439 **Figure 3. Heatmaps showing pixel-level change in BMD over 104 weeks in each**
440 **prosthesis group measured by DXA-RFA. Left 3 panels show percentage BMD change**
441 **at each timepoint after FDR correction. Right 2 panels show within group areas of**
442 **significant change (Q value). Between group analyses for areas of loss and gain are by**
443 **repeated measures ANOVA over 104 weeks.**

444

445 Figure 4. Graphs showing changes in serum concentrations of A) Carboxy-terminal
446 telopeptide of type I collagen (CTX), and B) Amino-terminal propeptide of type I
447 procollagen (PINP) in each prosthesis group over 104 weeks. Analysis is between group by
448 repeated-measures ANOVA **over 104 weeks.**

Table 1. Baseline demographic characteristics of completing participants. Values are mean \pm standard deviation. Analyses are between group by [†]Chi-squared test or [‡]t-test.

Variable	Tri-Lock Prosthesis (n=46)	Corail prosthesis (n=40)	p-value
Gender			
Male	22	17	
Female	24	23	0.621 [†]
Age in years	60.4 \pm 10.1	58.6 \pm 10.2	0.312 [‡]
BMI	27.4 \pm 2.9	27.6 \pm 2.5	0.859 [‡]
ASA class (Count, %)			
I	1	3	0.049 [†]
II	28	31	
III	17	6	
IV	0	0	
Baseline CTX (ng/ml)	0.425 \pm 0.193	0.403 \pm 0.186	0.609 [‡]
Baseline PINP (ng/ml)	54.47 \pm 21.39	55.92 \pm 10.82	0.753 [‡]
	Contralateral native hip (n=36)	Contralateral native hip (n=33)	
Total hip BMD (g/cm²)	1.01 \pm 0.14	1.01 \pm 0.148	0.966 [‡]
t-score total hip	-0.28 \pm 1.07	-0.25 \pm 0.99	0.889 [‡]
z-score total hip	0.40 \pm 1.18	0.39 \pm 0.90	0.953 [‡]

Table 2. Pixel-level bone mineral density changes in the Tri-Lock versus Corail Prosthesis groups over 104 weeks. Analysis is number of pixels with change/total number of pixels in Tri-Lock versus Corail group by Repeated Measures ANOVA after False Discovery Rate correction at 5%. †Indicates post-hoc p-value at interval timepoints.

Mean ± SD number of pixels/total per femur with significant BMD decrease			
Time	Tri-Lock	Corail	p-value
26 weeks	927/9460 (9.80%) ± 82	0/11115 (0.00%) ± 0	<0.001 [†]
52 weeks	661/9460 (6.99%) ± 67	504/11115 (4.53%) ± 76	<0.001 [†]
104 weeks	1295/9460 (13.69%) ± 73	1072/11115 (9.64%) ± 50	<0.001 [†]
ANOVA			<0.001
Mean ± SD number of pixels/total per femur with significant BMD increase			
Time	Tri-Lock	Corail	p-value
26 weeks	21/9460 (0.22%) ± 6	0/11115 (0.00%) ± 0	<0.001 [†]
52 weeks	61/9460 (0.64%) ± 7	67/11115 (0.60%) ± 6	0.002 [†]
104 weeks	122/9460 (1.29%) ± 11	374/11115 (3.36%) ± 40	<0.001 [†]
ANOVA			<0.001

Table 3. Radiographic outcomes of both prostheses by week 104. Values are mean \pm standard deviation. Analyses are between groups by t-test.

Radiographic variable	Tri-Lock prosthesis (n=46)	Corail prosthesis (n=40)	p-value
Mean global offset difference (mm)	0.02 \pm 5.13	-1.57 \pm 4.77	0.072
Mean leg length discrepancy (mm)	-0.09 \pm 1.82	0.73 \pm 1.86	0.028
Mean stem alignment angle (degrees, varus +, valgus -)	0.78 \pm 1.52	2.07 \pm 2.11	< 0.001
Mean linear bone resorption at calcar (mm)	0.78 \pm 0.94	0.65 \pm 0.92	0.451

Table 4. Patient-reported outcome measures in the Tri-Lock versus Corail groups at pre-operative baseline and at week 104. Values are mean \pm standard deviation. Analysis is: \dagger within group between baseline and week 104 by paired t-test, and $\dagger\dagger$ between group improvement in PROM score by independent t-test

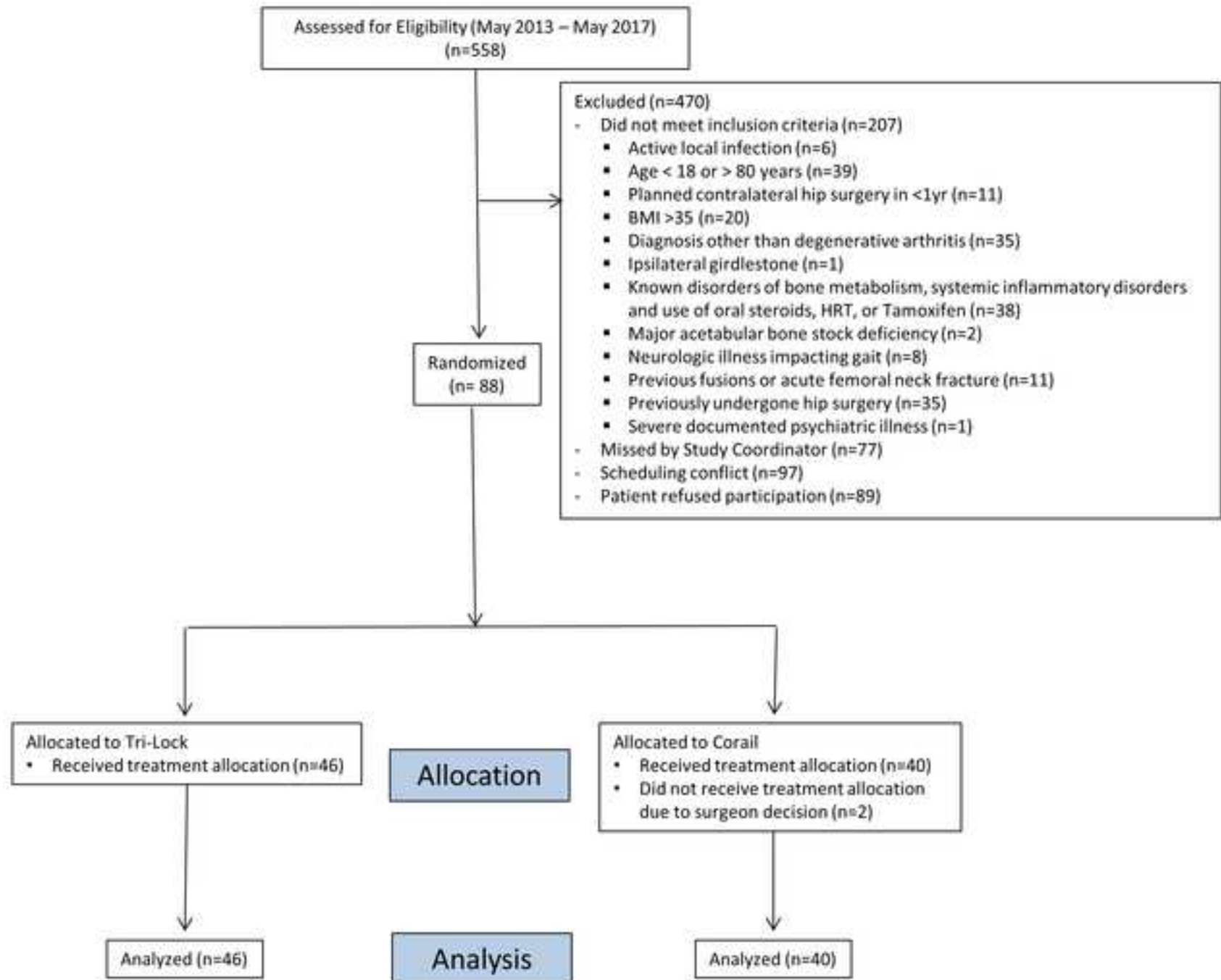
PROMs (mean \pm SD)	Tri-Lock Prosthesis (n= 46)	Corail prosthesis (n= 40)	p- value	$\dagger\dagger$p-value change scores between groups
Pre Harris Hip Score - Pain	17.5 \pm 7.19	19.2 \pm 7.12	0.231	0.728
Post Harris Hip Score - Pain	35.6 \pm 8.43	36.9 \pm 8.96	0.342	
\daggerp-value	<0.001	<0.001		
Pre Harris Hip Score - Function	27.7 \pm 7.64	29.9 \pm 6.83	0.167	0.132
Post Harris Hip Score - Function	42.0 \pm 5.77	42.6 \pm 7.40	0.275	
\daggerp-value	<0.001	<0.001		
Pre WOMAC - Pain	47.3 \pm 17.7	55.0 \pm 14.9	0.054	0.362
Post WOMAC - Pain	87.2 \pm 16.2	87.8 \pm 16.8	0.661	
\daggerp-value	<0.001	<0.001		
Pre WOMAC - Stiffness	43.8 \pm 20.7	45.0 \pm 19.2	0.518	0.890
Post WOMAC - Stiffness	78.5 \pm 21.5	82.6 \pm 22.0	0.284	
\daggerp-value	<0.001	<0.001		
Pre WOMAC - Function	47.0 \pm 17.1	58.4 \pm 17.7	0.007	0.876
Post WOMAC - Function	87.2 \pm 14.4	90.6 \pm 15.8	0.150	
\daggerp-value	<0.001	<0.001		
Pre UCLA	4.80 \pm 1.78	5.23 \pm 2.07	0.491	0.329
Post UCLA	6.26 \pm 1.89	6.24 \pm 2.16	0.654	

[†] p-value	<0.001	<0.001		
-----------------------------	--------	--------	--	--

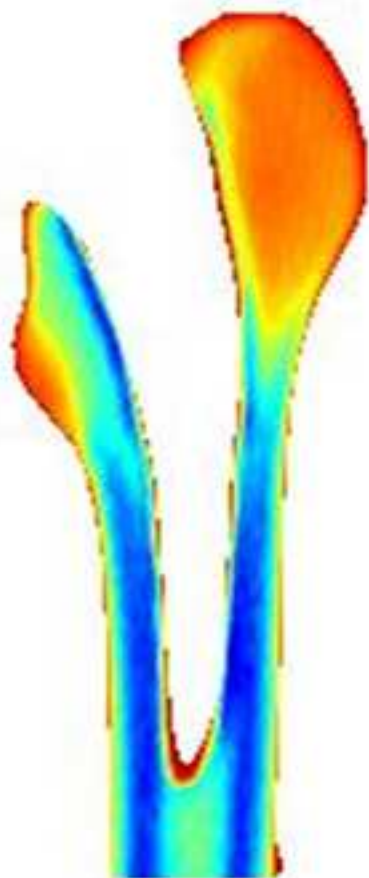
Table 5: Previous randomized controlled trials (2015-onwards) reporting on bone mineral density results of a variety of stem designs.

Study	No. of hips (n)	Comparison groups	Mean Follow-up	Results	Limitations
Schilcher et al (2017) ²⁸	60	Standard cementless femoral stem (Taperloc) vs. a 35-mm shorter version (Microplasty).	2-year	Greater bone loss around the shorter stem, although this was not statistically significant.	Underpowered to detect a significant difference in BMD between the prostheses.
Meyer et al (2019) ²⁹	140	Cementless bone preserving stem (Fitmore) vs. cementless straight stem (CLS Spotorno).	5-year	The bone-preserving Fitmore stem exhibited less proximal femoral bone loss than the CLS Spotorno conventional stem.	Different stem length of the 2 implants used with a modification to Gruen zones for better comparability.
Salemyr et al (2015) ³⁰	51	Ultra-short stem (Proxima) vs. conventional tapered stem (Bi-metric).	2-year	The conventional stem had greater bone loss (mainly in Gruen zones 1 and 7).	Lack of patient blinding. Possibly underpowered.
Freitag et al (2016) ³¹	144	Cementless bone preserving stem (Fitmore) vs. cementless straight stem (CLS Spotorno).	1-year	Although both designs had implant-specific stress-shielding, the Fitmore stem had less proximal femoral bone loss than the CLS Spotorno stem (at ROI 6).	Short follow-up.
Kim et al (2016) ³²	400	Ultrashort anatomic	12-year	BMD was greater in the ultrashort stem group than in	Difficulty at evaluating

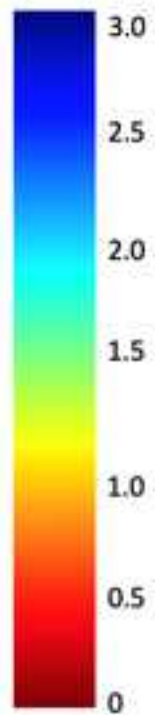
		cementless stem (Proxima) vs. conventional anatomic cementless stem (Profile)		the conventional stem group (mostly in zones 1 and 7).	longitudinal BMD changes using conventional DEXA of 2 different stem designs (e.g. slight changes in femoral rotation can affect precision of the measurement).
--	--	---	--	--	---



Tri-Lock



BMD in
grams/cm²



Corail

